International Journal of Computational Fluid Dynamics, Vol. 19, No. 7, October 2005, 493–500

Taylor & Francis
Taylor & Francis Group

Comparison of near-wall treatment methods for high Reynolds number backward-facing step flow

JAE -YONG KIM†, AFSHIN J. GHAJAR†*, CLEMENT TANG† and GARY L. FOUTCH‡

†School of Mechanical and Aerospace Engineering, Oklahoma State University, Stillwater, OK 74078, USA
‡School of Chemical Engineering, Oklahoma State University, Stillwater, OK 74078, USA

(Received 14 April 2005; revised 8 September 2005; in final form 11 November 2005)

A comparison of near-wall treatment methods using different turbulence models for flow over a backward-facing step is presented. A Reynolds number (*Re*) of about 38,000 ($U_\infty = 44.2$ m/s), based on the step height and the mean stream velocity, was considered. An appropriate near-wall treatment method is critical to the choice of turbulence model used to predict wall-bounded flow. Predictions were obtained by applying standard wall functions, non-equilibrium wall functions and a two-layer model with six different turbulence models. These results were compared with data by Driver and Seegmiller ("Backward-facing step with inclined opposite wall—experiments by driver and seegmiller", 1985a, http://cfd.me.umist.ac.uk/ercoftac [2003, Jan 31]). Non-equilibrium wall functions with modified $k - \varepsilon$ models predicted the closest reattachment length. However, the two-layer model gave results more representative of the entire flow pattern. The predictions show that a proper combination of turbulence models and near-wall treatment methods give reliable results.

Keywords: Backward-facing step flow; Turbulence models; Near-wall treatment methods; Wall functions

Nomenclature

C_μ	constant (≈ 0.09)
C_f	skin-friction [$= \tau_w/(0.5\rho U_\infty^2)$]
C_p	pressure coefficient [$= (p - p_\infty)/(0.5\rho U_\infty^2)$]
h	step height, figure (1), m
h_{duct}	duct height before step, m
H	duct height after step, figure (1), m
k	turbulence kinetic energy, m^2/s^2
l	mixing length, m
L_R	reattachment length, figure (1), m
p	pressure, Pa
Re	Reynolds number, ($= \rho U_\infty h/\mu$)
U	streamwise component of mean velocity, m/s
U_τ	friction velocity, ($= \sqrt{\tau_w/\rho}$), m/s
U_∞	freestream reference velocity, (= 44.2 m/s)
x	distance from step, figure (1), m
y	normal distance from the wall at the cell center, m
y^+	non-dimensional distance from the wall in wall coordinates ($= yU_\tau/\nu$)

Greeks

α	wall angle, figure (1), deg
δ	boundary layer thickness, m
ε	turbulent dissipation rate, m^2/s^3
κ	von Kármán constant [≈ 0.42]
μ	dynamic viscosity, kg-m/s
ν	kinematic viscosity, m^2/s
ρ	density, kg/m^3
τ	shear stress, N/m^2
ω	specific dissipation rate, s^{-1}

Subscripts

∞	free stream
NW	at the near wall
w	at the wall

Abbreviations

RKE	realizable $k - \varepsilon$ model
RNG	renormalization group $k - \varepsilon$ model
RSM	Reynolds stress model
SKE	standard $k - \varepsilon$ model
SKW	standard $k - \omega$ model
SST	shear-stress transport $k - \omega$ model

*Corresponding author. Tel.: +1-405-744-5900. Fax: +1-405-744 7873. Email: ghajar@ceat.okstate.edu

International Journal of Computational Fluid Dynamics
ISSN 1061-8562 print/ISSN 1029-0257 online © 2005 Taylor & Francis
http://www.tandf.co.uk/journals
DOI: 10.1080/10618560500502519

1. Introduction

The backward-facing step due to its relative simplicity is one of the most popular geometries used to evaluate turbulence models for separated flows. Many investigators have compared predictions by either well-known or their own turbulence models to available data (Driver and Seegmiller 1985b, Avva 1988, Kim and Choudhury 1995, Rhee and Sung 2000). The accuracy of the predicted reattachment location of the flow is often used as a method to evaluate the performance of the turbulence models.

In practice, the backward-facing step in wall-bounded turbulent flow is common; such as in pipes, channels and over wings and bodies in flight and around ships. However, irregardless of the magnitude of the flow Reynolds number (*Re*) away from the wall, these wall-bounded flows are significantly affected by several conditions, such as no-slip at the wall, viscous damping on tangential velocity, kinematic blocking on the normal fluctuations, the large gradients in mean velocity near the wall and flow separation. Therefore, in order to predict the wall-bounded turbulent flow successfully, the near-wall treatment method should be evaluated carefully. Limited literature discusses the effect of the near-wall treatment methods on predictions, and the importance of these methods is often overlooked.

In this study, we have focused on the performance of near-wall treatment methods which are widely available through literature and commercial computational fluid dynamics (CFD) packages. We have selected three near-wall treatments—two methods are based on wall functions and the third is a two-layer model—and linked these to different turbulence models in order to compare high *Re* backward-facing step flow with experimental data of Driver and Seegmiller (1985a). The focus of this paper is on the validation of near-wall treatment methods rather than turbulence models, even though the results are presented and discussed with several turbulence models.

2. Background

In order to compute the flow over the backward-facing step, a commercial CFD package, FLUENT™, is used. FLUENT is capable of solving the full steady-state and transient Navier–Stokes equations using a finite volume method in two dimensional (2D) or three dimensional (3D) geometries. For turbulent flows, the Spalart–Allmaras model, $k-\varepsilon$ models, $k-\omega$ models, Reynolds stress model (RSM) and large eddy simulation model are provided.

The turbulence models used in this study are the standard $k-\varepsilon$ model (SKE), renormalization group $k-\varepsilon$ model (RNG), realizable $k-\varepsilon$ model (RKE), RSM, standard $k-\omega$ model (SKW) and shear-stress transport $k-\omega$ model (SST). The near-wall treatment methods used in this study for SKE, RNG, RKE and RSM models are standard wall functions, non-equilibrium wall functions and two-layer model. The detailed descriptions for all three near-wall treatments and turbulence models may be found in FLUENT User's Guide (2003).

The standard wall functions are based on the proposal of Launder and Spalding (1974), and have been widely used for industrial flow. Kim and Choudhury (1995) proposed the use of the non-equilibrium wall functions in order to improve the accuracy of the standard wall functions. The key elements in non-equilibrium wall functions are pressure-gradient sensitized Launder and Spalding (1974) log–law for mean velocity and the two-layer-based concept to compute the turbulence kinetic energy in the wall-adjacent cells. In the two-layer model, the whole domain is subdivided into a viscosity-affected region and a fully-turbulent region. The one-equation model of Wolfstein (1969) is employed in the viscosity-affected region. In the fully turbulent region, the $k-\varepsilon$ models or RSM are employed.

The $k-\omega$ model is based on transport equation for the turbulence kinetic energy, k and the specific dissipation rate, ω, which can also be thought of as the ratio of ε to k (Wilcox 1998). In FLUENT, users have the option of using either the SKW or the SST. The wall boundary conditions for the turbulence kinetic energy, k equation in the $k-\omega$ models are treated in the similar way as the k equation is treated when the $k-\varepsilon$ models is used with the two-layer model (FLUENT 2003a).

3. Problem description and setting

Figure 1 shows the geometry of the backward-facing step and flow configuration. The test configuration of Driver and Seegmiller (1985a) has a large tunnel-width to step-height ratio of 12 to minimize 3D effects in the separated region, and a small expansion ratio $[(h_{\text{duct}}+h)/h_{\text{duct}}=1.125]$ to minimize the free-stream pressure gradient owing to sudden expansion. The experiments were conducted in a controlled environment on the tunnel floor of a low-speed wind tunnel facility, where the z-velocity component was minimized (Driver and Seegmiller 1985a). Hence, their data can be compared with a 2D computational model. Driver and Seegmiller (1985a) reported their experimental uncertainties in terms of C_{p} and C_{f}. Uncertainties in C_{p} were assessed to be ± 0.009 (with 95% confidence limits), and uncertainties in C_{f} were assessed to be $\pm 8\%$ for a 95% confidence level and $\pm 15\%$ in the separated region.

In this study, the comparisons were performed for 0 and 6° wall-angles. The computation domain starts from an inlet located $4.0h$ ($h=0.0127$ m) upstream from the step. The outlet boundary is placed at $30h$ downstream from the step for 0° wall-angle and at $38h$ downstream from the step for 6° wall-angle, respectively, and the

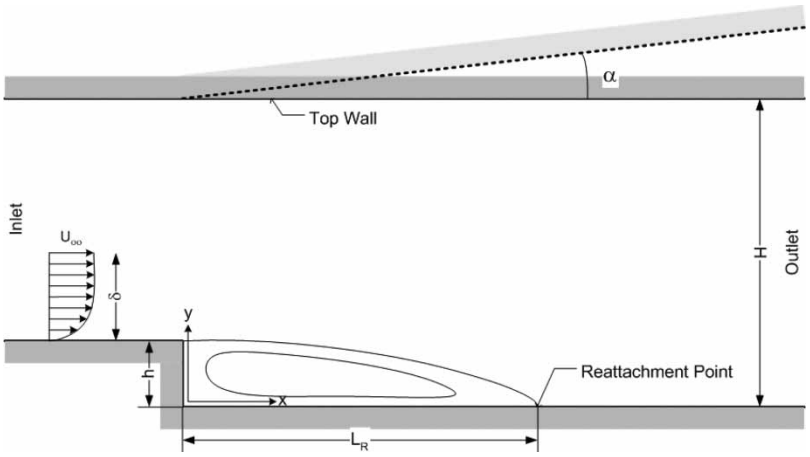

Figure 1. Backward-facing step.

height of upstream channel is 8*h*. The *Re* based on the step height and free-stream velocity is about 38,000.

The inlet boundary conditions are specified as three profiles of *x*-velocity, turbulent kinetic energy and dissipation rate. The profiles approximate fully developed conditions. The procedures to set the inlet boundary conditions described in this section are according to the information posted in www.fluent.com (2003b, June 18).

The 1/7th power law is used to specify the streamwise component of mean velocity:

$$U = U_\infty \left(\frac{y}{h_{\text{duct}}/2}\right)^{1/7} \tag{1}$$

The turbulent kinetic energy is assumed to vary linearly from a near wall value of

$$k_{\text{NW}} = \frac{U_\tau^2}{\sqrt{C_\mu}} \tag{2}$$

to a free-stream value of

$$k_\infty = 0.002 U_\infty^2 \tag{3}$$

The dissipation rate is given by

$$\varepsilon = C_\mu^{3/4} \left(\frac{k^{3/2}}{l}\right) \tag{4}$$

where l is the minimum of κy and $0.085 h_{\text{duct}}/2$ ($\kappa = 0.42$).

At the outlet, zero-diffusion condition was applied. The wall boundaries were applied with no-slip condition and smooth wall condition. The flow was assumed incompressible.

Several quadrilateral meshes of varying resolutions were employed to establish the mesh-independency of the solutions. The meshes used for presented computations for the flow over backward-step are partially shown in figure 2 and summarized in table 1. Figure 2a shows the mesh for wall functions, namely the standard wall functions and the non-equilibrium wall functions; and figure 2b shows the mesh for the two-layer model. In FLUENT, users are not given the option for choosing the near-wall treatment methods in both SKW and SST models; hence the SKW and SST models were computed with both mesh for wall functions (figure 2a) and mesh for two-layer model (figure 2b).

4. Results and discussion

4.1 Reattachment length

The predicted reattachment lengths are shown in table 2 according to the turbulence models and the near-wall

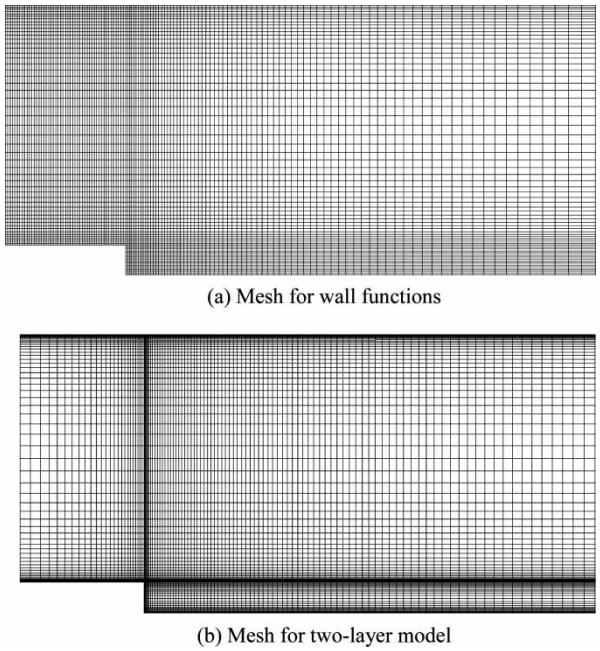

Figure 2. Meshes for the backward-facing step with 0° wall-angle.

Table 1. Meshes for the backward-facing step model.

	Wall functions		Two-layer model	
	$\alpha = 0°$	6°	0°	6°
Cell numbers	9000 (100 × 90)	8000 (100 × 80)	17,352 (177 × 98)	15,003 (150 × 100)
y^+	<43	<32	<1.25	<0.95

treatment methods with measured values by Driver and Seegmiller (1985a). As given in table 2, the predicted reattachment lengths by standard wall functions are under-predicted by 7.3–28% regardless of the applied turbulence model for both 0 and 6° wall-angles.

For the cases employing non-equilibrium wall functions, RNG and RKE models predicted the reattachment lengths within 2.4% of the measurement for both 0 and 6° wall-angles. However, SKE and RSM models with non-equilibrium wall functions under-predicted the reattachment lengths for both wall-angles by 7.3–22%.

The two-layer model under-predicted the reattachment lengths for the cases with SKE and RSM by 8.1–16% for both 0 and 6° wall-angles. For RNG and RKE with two-layer model, the reattachment lengths are over-predicted by 3.0–7.8% for both wall-angles.

The SKW model computed with the mesh for wall functions (figure 2a) over-predicted the reattachment lengths by 8.6–14% for both 0 and 6° wall-angles. However, the SST model computed with the mesh for wall functions predicted the reattachment lengths within 2.4% for both wall-angles. When SKW model is computed with the mesh for two-layer model (figure 2b), the reattachment lengths are over-predicted by 21% for both wall-angles. The SST model computed with the mesh for two-layer model over-predicted the reattachment lengths by 4.6–16% for both wall-angles.

Overall, RNG and RKE with non-equilibrium wall functions and SST with the mesh for wall functions showed the best results to predict the reattachment lengths based on the measured values.

4.2 Skin friction and pressure coefficient

Figures 3 and 4 show the comparisons of the predicted skin-friction, C_f, and the predicted static pressure coefficient, C_p, on the bottom wall with the data measured by Driver and Seegmiller (1985a) for 0 and 6° wall-angles, respectively. For the case of 0° wall-angle, as shown in figure 3, the standard wall functions predicted the C_f for $x/h \geq 8$ within 38% regardless of the turbulence model. The non-equilibrium wall functions predicted the C_f for $x/h \geq 8$ within 31% and the two-layer model predicted the C_f for $x/h \geq 8$ within 52%, regardless of the turbulence model. SKW and SST computed with the mesh for wall functions predicted the C_f for $x/h \geq 8$ within 50%; and with the mesh for two-layer model, SKW and SST under-predicted the C_f for $x/h \geq 8$ by 5.3–76%. Overall, for 0° wall-angle, RNG and RKE with non-equilibrium wall functions showed the best results by predicting C_f for $x/h \geq 8$ within 10%. In addition, the predicted C_p regardless of turbulence models and the near-wall treatment methods are over-predicted by 7.0–44% for $x/h \geq 8$.

For the case of 6° wall-angle, as shown in figure 4, the accuracy of the predicted C_f dropped compared to

Table 2. Comparison of the reattachment lengths.

	Near-wall treatment methods			
Turbulence models	Standard wall functions	Non-equilibrium wall functions	Two-layer model	Measured (1985a)
Reattachment length (L_R/h) for 0° wall-angle				
SKE	4.9–5.1	5.3–5.5	5.7–5.8	6.26 ± 0.10
RNG	5.7–5.9	6.1–6.3	6.4–6.5	
RKE	5.7–5.9	6.1–6.3	6.6–6.7	
RSM	5.1–5.3	5.7–5.9	5.6–5.7	
SKW		6.7–6.9	7.5–7.6	
SST		6.1–6.3	6.5–6.6	
Reattachment length (L_R/h) for 6° wall-angle				
SKE	5.9–6.1	6.3–6.6	7.0–7.1	8.30 ± 0.15
RNG	7.4–7.6	8.0–8.2	8.5–8.6	
RKE	7.4–7.6	8.0–8.2	8.9–9.0	
RSM	5.9–6.1	6.8–7.1	6.9–7.0	
SKW		9.4–9.6	10.1–10.2	
SST		8.4–8.6	9.6–9.7	

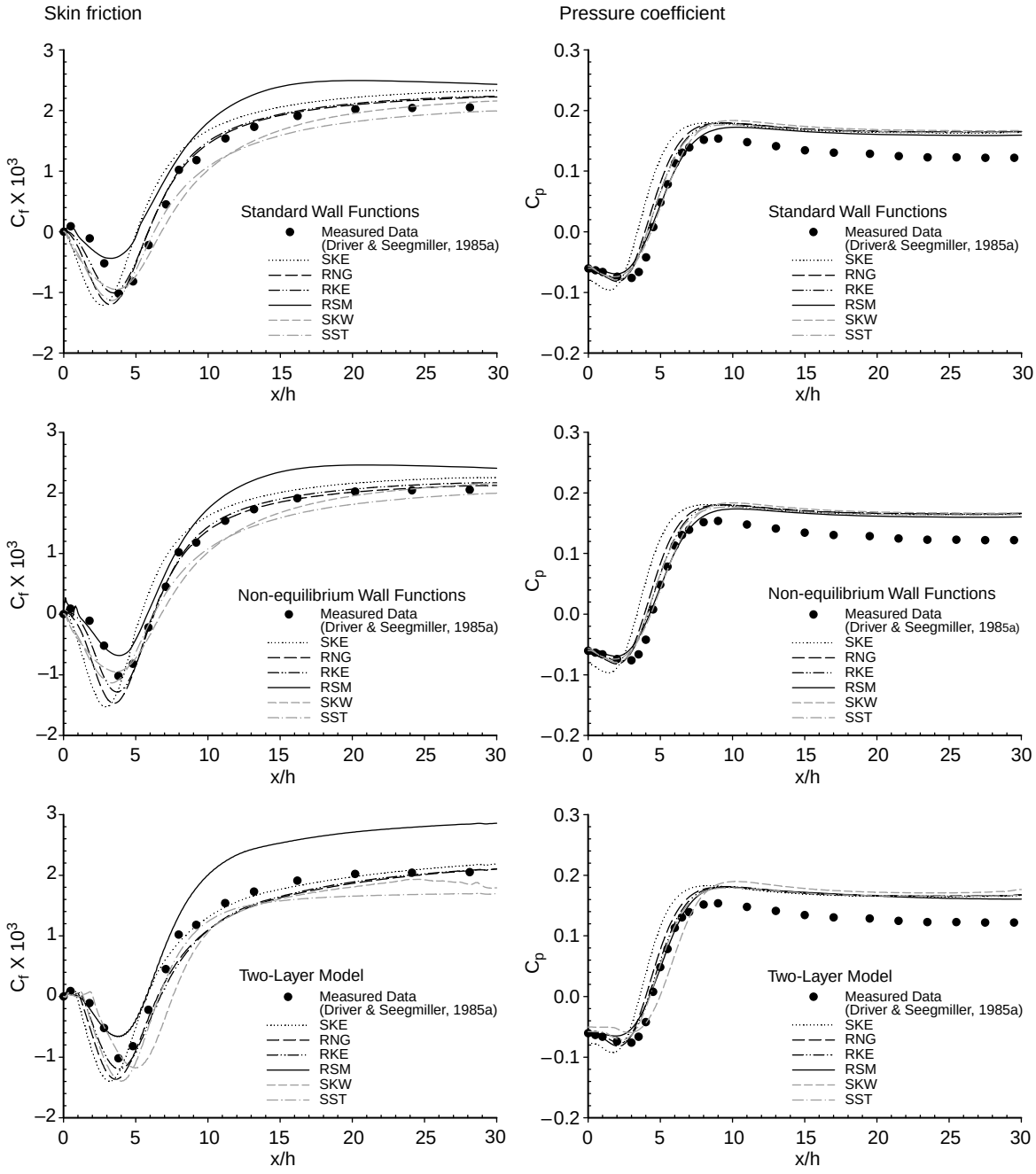

Figure 3. Comparison of C_f and C_p for different turbulence models and near-wall treatments ($\alpha = 0°$, $Re = 38{,}000$).

the case of 0° wall-angle. The standard wall functions predicted the C_f for $x/h > 10$ within 102% regardless of the turbulence model. The non-equilibrium wall functions predicted the C_f for $x/h > 10$ within 83% and the two-layer model predicted the C_f for $x/h > 10$ within 101%, regardless of the turbulence model. SKW and SST computed with the mesh for wall functions under-predicted the C_f for $x/h > 10$ by 22–52%; and with the mesh for two-layer model, SKW and SST under-predicted the C_f for $x/h > 10$ by 18–101%. Overall, for 6° wall-angle, RNG and RKE with non-equilibrium wall functions showed the best results by predicting C_f for $x/h > 10$ within 24%. In addition, the predicted C_p regardless of turbulence models and the near-wall treatment methods are over-predicted by 7.0–22% for $x/h > 10$, which is better when compared to the case of 0° wall-angle.

4.3 Velocity profiles and velocity vectors

The mean velocity profiles predicted by all three near-wall treatment methods, shown in figure 5 for 0°

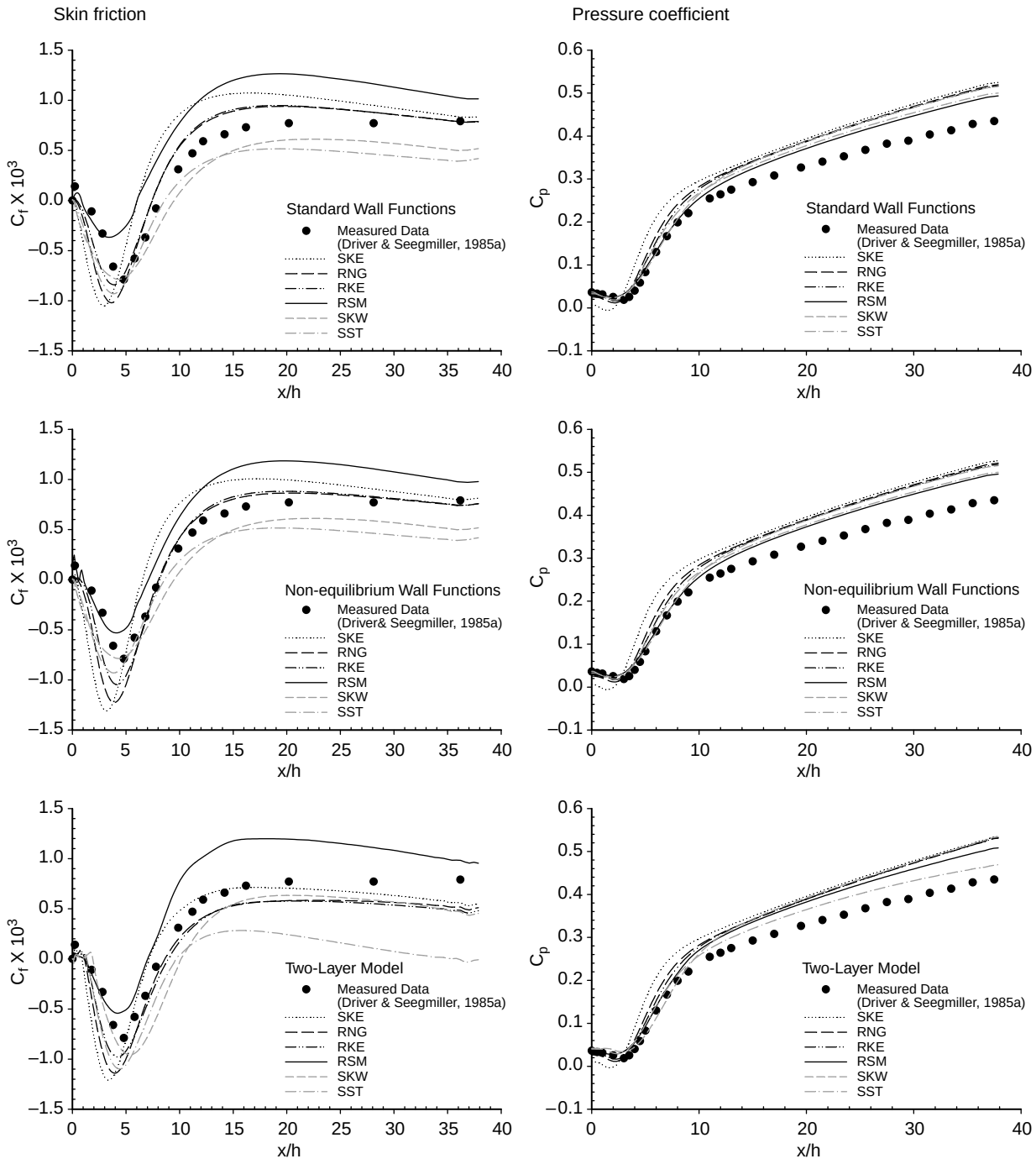

Figure 4. Comparison of C_f and C_p for different turbulence models and near-wall treatments ($\alpha = 6°$, $Re = 38{,}000$).

wall-angle, are almost identical with one another and with the experimental measurements. Likewise, for the 6° wall-angle, the mean velocity profiles predicted by all three near-wall treatment methods are almost identical with one another and the experimental measurements (not shown here). Note that the velocity profile at the inlet is assumed fully developed with $U_\infty = 44.2$ m/s. For comparison, in the experiments of Driver and Seegmiller (1985a), the inlet conditions were $U_\infty = 44.2$ m/s and $\delta = 0.019$ m.

Figure 6 shows the velocity vectors in the corner with 0° wall-angle. As shown in the figures, the recirculation observed in the experiments is captured in the cases of RSM regardless of near-wall treatment methods used. The SKE, RNG and RKE models failed to capture the recirculation when computed with wall functions. In addition, figure 6e and f shows that both

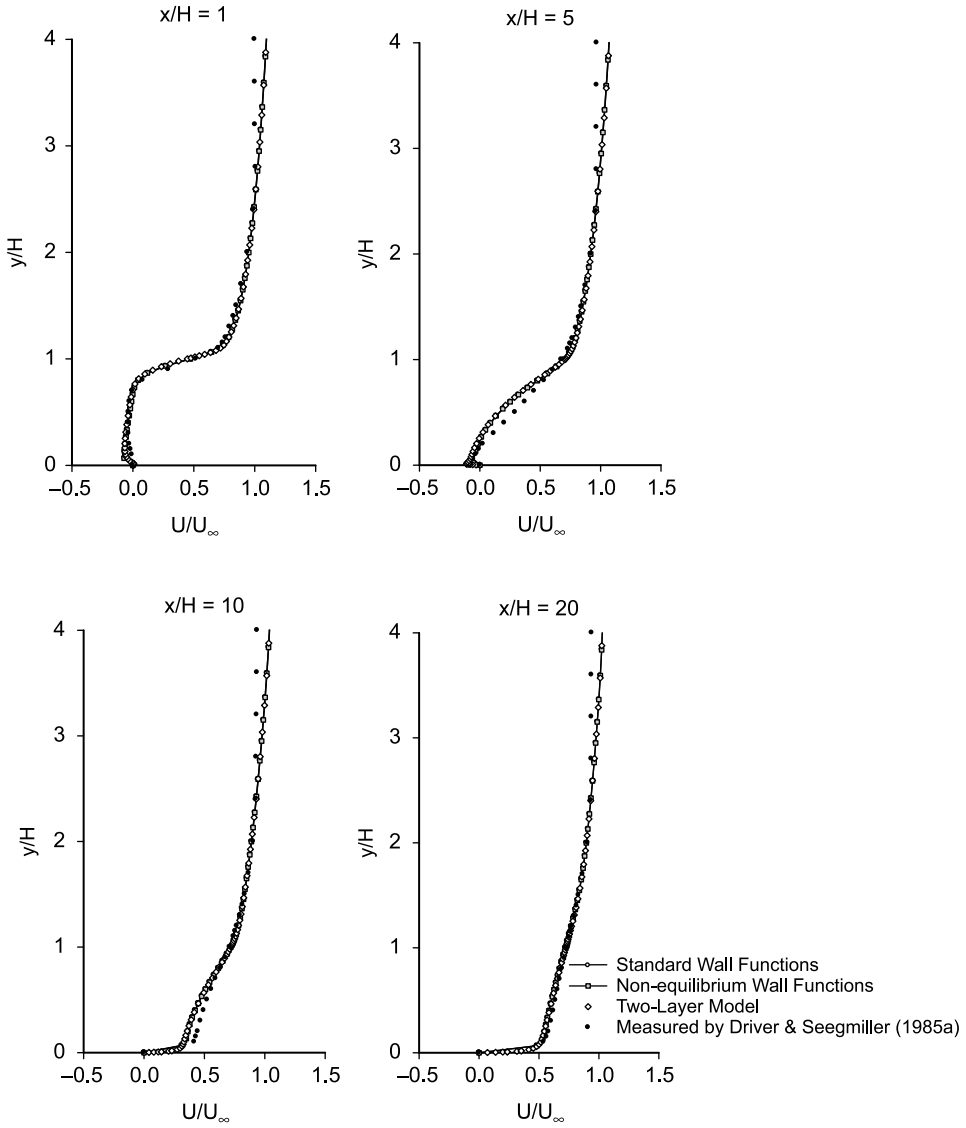

Figure 5. Comparison of velocity profiles for RNG $k-\varepsilon$ turbulence model with different near-wall treatments ($\alpha = 0°$, $Re = 38{,}000$).

SKW and SST models computed with the mesh for wall functions were also unable to capture the recirculation. However, the two-layer model when used with any turbulence model gives more physically meaningful velocity vectors, such as recirculation in the corner.

5. Conclusions

This paper provides a useful validation study for a range of near-wall treatment methods and turbulence models for the backward-facing step flow. The performance of standard wall functions, non-equilibrium wall functions and two-layer models with six different turbulence models (SKE, RNG, RKE, RSM, SKW and SST) were compared with the measurements for high *Re* backward-facing step flow. The computational results were clearly affected by which combination of near-wall treatment method and turbulence model was used. In this study, non-equilibrium wall functions with RNG and RKE models showed the best results to predict the reattachment length, skin-friction and static pressure coefficient based on the measured values for both 0 and 6° wall-angles. The two-layer model when used with any turbulence model gives more physically meaningful velocity vectors; but predicted poorly when compared with measured values, even though the computational cost was expensive compared to the method of wall functions. This study showed that in order to accurately predict all of the flow features for a backward-facing step, a proper combination of near-wall treatment methods and turbulence models should be used.

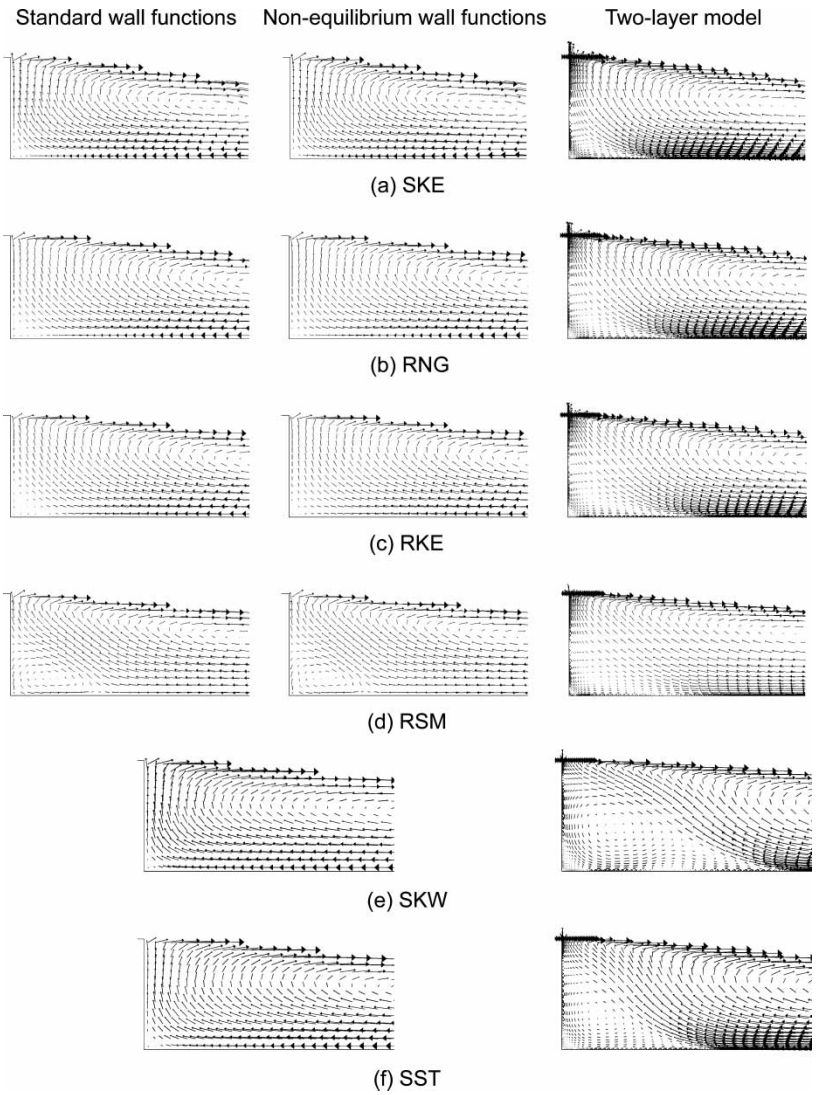

Figure 6. Comparison of velocity vector distributions in the corner of flow over backward-facing step predicted by different turbulence models and near-wall treatments ($\alpha = 0^{\circ}$, $Re = 38{,}000$).

References

Avva R.K., Computation of the turbulent flow over a backward-facing step using the zonal modeling approach. PhD Thesis, Stanford University, CA, 1988.

Driver, D.M. and Seegmiller, H.L., Backward-facing step with inclined opposite wall—experiments by driver and seegmiller, 1985a, WWW. URL http://cfd.me.umist.ac.uk/ercoftac [2003, Jan 31].

Driver, D.M. and Seegmiller, H.L., Features of a reattachment turbulent shear layer in divergent channel flow. *AIAA J.*, 1985b, **23**(2), 163–171.

FLUENT, Inc., *FLUENT 6.1 User's Guide*, 2003, (Lebanon: NH).

FLUENT, Inc., On the WWW URL http://www.fluent.com [2003, June 18].

Kim, S.-E. and Choudhury, D., A near-wall treatment using wall functions sensitized to pressure gradient. *ASME FED Separated and Complex Flows. ASME*, 1995, **217**, 273–279.

Launder, B.E. and Spalding, D.B., The numerical computation of turbulent flows. *Comp. Meth. Appl. Mech. Eng.*, 1974, **3**, 269–289.

Rhee, G.H. and Sung, H.J., A nonlinear low-reynolds number heat transfer model for turbulent separated and reattaching flows. *Int. J. Heat Mass Trans.*, 2000, **43**, 1439–1448.

Wilcox, D.C., *Turbulence Modeling for CFD*, 1998 (DCW Industries, Inc: La Canada, CA).

Wolfstein, M., The velocity and temperature distribution of one-dimensional flow with turbulence augmentation and pressure gradient. *Int. J. Heat Mass Trans.*, 1969, **12**, 301–318.